Video Article

Spatial Measurements of Perfusion, Interstitial Fluid Pressure and Liposomes Accumulation in Solid Tumors

Shawn Stapleton[1,2,3], Daniel Mirmilshteyn[2], Jinzi Zheng[3,4], Christine Allen[2,4,5], David A. Jaffray[1,2,3,4,5,6]

[1]Department of Medical Biophysics, University of Toronto

[2]Leslie Dan Faculty of Pharmacy, University of Toronto

[3]STTARR Innovation Centre, Princess Margaret Cancer Centre

[4]Institute of Biomaterials and Biomedical Engineering, University of Toronto

[5]Techna Institute, University Health Network

[6]Radiation Medicine Program, Princess Margaret Cancer Centre

Correspondence to: Shawn Stapleton at Shawn.Stapleton@rmp.uhn.ca

Abstract

The heterogeneous intra-tumoral accumulation of liposomes is a critical determinant of their efficacy. Both the chaotic tumor microcirculation and elevated IFP are linked to the heterogeneous intra-tumoral distribution of nanotechnology-based drug delivery systems such as liposomes. In the present study, the relationship between tumor microcirculation, elevated IFP, and accumulation of nanoparticles was investigated through *in vivo* experimentation. This was accomplished by evaluation of the tumor microcirculation using dynamic contrast enhanced computed tomography (DCE-CT) and measurement of tumor IFP using a novel image-guided robotic needle placement system connected to the micro-CT scanner. The intra-tumoral accumulation of liposomes was determined by CT image-based assessment of a nanoparticle liposomal formulation that stably encapsulate the contrast agent iohexol (CT-liposomes). CT imaging allowed for co-localization of the spatial distribution of tumor hemodynamics, IFP and CT-liposome accumulation in an individual subcutaneous xenograft mouse model of breast cancer. Measurements led to the discovery that perfusion and plasma volume fraction are strong mediators of the intra-tumoral distribution of liposomes. Furthermore, the results suggest that IFP plays an indirect role in mediating liposome distribution through modulating blood flow.

Video Link

The video component of this article can be found at http://www.jove.com/video/54226/

Introduction

Measuring the intra-tumoral accumulation of nanoparticle drug delivery systems may provide an important tool to determine if an adequate concentration of cytotoxic drug has been achieved within the tumor. The development of "image-able" liposomal systems allows for non-invasive and quantitative *in vivo* detection of the drug delivery vehicle using imaging modalities such as positron emission tomography (PET)[1], optical fluorescence[2], and computed tomography (CT)[3,4] and magnetic resonance imaging (MRI)[5]. Imaging has been used to determine the pharmacokinetics and biodistribution of liposome delivery systems and to reveal the extent of inter-subject and intra-tumoral heterogeneity in nanoparticle accumulation[6,7]. However, imaging of nanoparticles alone does not identify the biological barriers that have contributed to their poor accumulation and distribution. This knowledge is paramount to the rational development of more efficacious formulations, and strategies to improve intra-tumoral accumulation[8]. It has been demonstrated that therapeutic strategies can be applied to modulate specific biological barriers resulting in improved nanoparticle transport[9]. Additionally, nanoparticle formulations have been developed to specifically overcome specific biological transport barrier[10]. In both scenarios, measurements of biological barriers could be used to guide the use of an appropriate nanoparticle drug delivery strategy.

Tumor microcirculation and elevated IFP are believed to be two key determinants of the intra-tumoral accumulation of nanoparticles, such as liposomes, in solid tumors[9,11]. However, other barriers that to contribute to poor liposome accumulation include a dense extracellular matrix, impermeable vasculature, and solid tissue pressure[12]. These barriers are related in a spatio-temporal manner, with abnormal blood flow and elevated interstitial fluid pressure being two important factors driving the initial delivery and extravasation of nanoparticles. As previously discussed, establishing the relationship between the tumor microcirculation, elevated IFP, and the intra-tumoral accumulation of liposomes is imperative for proper interpretation of liposome imaging data. Herein quantitative methods to measure the relationship between the tumor microcirculation, elevated IFP, and nanoparticle accumulation in a solid tumor are presented. This is accomplished by performing co-localized measurements of the intra-tumoral distribution of a CT liposome contrast agent using volumetric CT imaging, tumor microcirculation using

dynamic contrast enhanced computed tomography imaging, and tumor IFP using an image-guided robotic needle positioning system, termed the CT-IFP robot[13].

Protocol

All *in vivo* experiments were performed under a protocol approved by the University Health Network Institutional Animal Care and Use Committee.

1. Animal Model

1. Culture between 5 to 7 x 10^6 MDA-MB-231 breast adenocarcinoma tumor cells in DMEM together with 10% Fetal Bovine Serum (FBS) and 100x dilution of penicillin-streptomycin.
2. Harvest cells when they are 80% confluent using a 0.05% trypsin-EDTA solution. After 3-5 min neutralize trypsin-EDTA with a 3x volume of DMEM. Take a 15 µl aliquot of cells and count using a hemocytometer. Centrifuge cells into a pellet for 5 min at 200 x g, and re-suspend in HBS at a concentration of 10 x 10^6 cells per ml.
3. Implant subcutaneous (SC) tumors by injecting 1 to 2 x 10^6 cells in the hind limb of each 8 to 12 week old female SCID mouse (n = 5). Use a standard 25 G needle for injection.
4. Monitor tumor growth using calipers (Volume = 0.5 x Length x Width^2) and start the measurements once the SC tumors have reached a volume >200 mm^3 (approximately 7 to 9 days).

2. CT-liposome Preparation and Characterization

1. Liposome Preparation
   1. Dissolve lipid components (200 mmol/L) for the CT-liposomes, including 1,2-dipalmitoyl-sn-glycero-3-phosphocholine (DPPC), cholesterol (CH), and 1,2-distearoyl-sn-glycero-3-phosphoethanolamine-N-poly(ethylene glycol) 2000 (DSPE-PEG2000) in anhydrous ethanol at 70 °C at a molar ratio of 55:40:5 DPPC:CH:DSPE-PEG2000.
   2. Evaporate ethanol by maintaining heat at 70 °C, then add the CT contrast agent iohexol (300 mg/ml of iodine) to the solution such that the final lipid concentration is 100 mM.
   3. Maintain the solution at 70 °C for 4 hr with frequent vortexing.
   4. To obtain unilamellar vesicles, extrude the sample 5 times through two stacked 200 nm pore size membranes at a pressure of 250 psi and extrude again by 5 cycles through two stacked 80 nm pore size membranes at 400 psi using a 10 ml lipid extruder. Pipette a volume of 10 ml of liposomes into the extruder at the beginning of each extrusion cycle and collect into a sterile conical tube or glass vial after each extrusion cycle.
   5. Remove the un-encapsulated iohexol by 16 hr of dialysis using a 100 kDa molecular weight cut off (MWC) dialysis bag against a 250-fold volume excess of 0.02 mM HEPES-buffered saline solution (HBS, pH 7.4). For example, place 1 ml of liposome solution inside the dialysis bag with 250 ml of HBS outside the bag in a beaker.
   6. Concentrate the CT-liposomes using a 750,000 nomical MWC commercial tangential flow system according to the manufacturer's instructions. Concentrate to a final iodine concentration of approximately 55 mg ml^{-1}.

2. Liposome Characterization
   1. Measure encapsulation efficiency by rupturing the CT-liposomes using a 10-fold volume excess of ethanol to release the ioxehol and then dilute using a 100-fold volume excess of deionized water (*i.e.* 10 µl of liposomes ruptured using 100 µl of ethanol and then diluted to a final volume of 10 ml).
   2. Determine iohexol concentration using a UV spectrometer with detection at a wavelength of 245 nm. Calculate the encapsulations efficiency by taking the ratio amount of released iohexol agent to the amount of agent added during preparation.
   3. Measure the hydrodynamic diameter and zeta potential using a dynamic light scattering particle size analyzer system according to the manufacturer's instructions. Dilute the CT-liposome solution by 200x (*i.e.* 5 µl of liposome in 1 ml of final volume) in deionized water to facilitate measurements.

3. CT Imaging of Tumor Microcirculation and CT-liposome Distribution

NOTE: Follow the manufacturer's instructions for performing a volumetric scan if different software version or equipment is used.

1. Anesthetize each mouse using 2% isoflurane mixed with medical air or oxygen and confirm by pinching the toe and observing no reaction. Apply ointment to the eyes to prevent dryness while under anesthesia. Immobilize animal in a prone position by taping paws to a thin plastic board.
2. Place a custom 27 G catheter, connected to 20 cm on PE10 tubing, into the lateral tail vein and secure in place with several pieces of tape.
3. Prepare a 1 ml syringe to contain at least 200 µl of the CT-liposomes. Prepare a 1 ml syringe with saline to use to flush the catheter. Finally, prepare a 1 ml syringe with at least 150 µl of free iohexol mixed with saline (9:1 ratio by volume).
4. Place the mouse prone on the micro-CT scanner bed. Use the laser positioning system to place the tumor in approximately the same orientation for each scan.
5. Place the CT-liposome syringe in a syringe pump and attach the catheter to the syringe. Set the pump rate of 10 µl per sec.
6. Initialize the system by performing a bright-dark calibration scan using the CT-scanner console software. Select the bright-dark scan option for each imaging protocol of interest, select bright-dark from the drop down menu and press the scan button to initiate the calibration.
7. Perform a volumetric anatomical micro-CT of the tumor prior to any contrast agent injection. Look at the CT scanner console software indicator to ensure the CT-scanner safety interlocks have been cleared. On the CT scanner console select scan select an x-ray energy of 80 kV, a tube current of 70 mA, and captures 1,000 image projections over time 16 sec. Press the scan button to initiate the scan.

8. Use the syringe pump to inject a bolus of CT-liposomes at a concentration of 400 mg iodine kg^{-1}. Set the pump to inject a volume of approximately 150 µl (assuming a 25 g mouse). Press the 'start' button on the pump to inject. Manually flush the catheter with 50 µl of saline (twice the volume of the catheter) to ensure the entire agent amount was injected and the catheter is clear.
9. Wait 10 min after the injection of CT-liposomes and then perform a second anatomical scan using the same method and settings described in 3.5.
10. Perform a DCE-CT scan by setting the syringe pump to inject a volume of 100 µl of the free iohexol mixed with saline (9:1 ratio by volume) using the same injection rate setting described in 3.3.
    1. On the CT-scanner console select the 5 min dynamic scan that uses an x-ray energy setting of 80 kV, a tube energy of 90mA, and captures 416 image projections every sec for the first 30 sec and followed by an acquisition every 10 sec. Capture 5 sec of DCE-CT data and then press the start button on the injection pump.
    2. After the DCE-CT scan perform a volumetric anatomical micro-CT scan.

11. Capture anatomical CT images between 48 and 72 hr post-injection of CT-liposomes, using the same volumetric CT settings as described in steps 3.5.
12. Reconstruct the anatomical CT and DCE-CT data using the GPU-reconstruction software.
    1. Load the image into the reconstruction software. Select the region of interest to be reconstructed by drawing an ROI over the image using a mouse. Set the save location and filename for the reconstructed imaged and select the output file type as '.mat'.
        NOTE: The software will automatically set the reconstructed voxel size to 0.153 x 0.153 x 0.153 mm^3 for anatomical scans and 0.153 x 0.153 x 0.462 mm^3 for DCE-CT scans. Click the 'begin reconstruction' button.

13. Use the pre-injection and 10 min post-injection scans of the CT-liposome to calculate the plasma volume fraction as previously described[3]. Furthermore, use the pre-injection and 5 min post-injection scans of iohexol to calculate the interstitial volume fraction as previously described[7].
14. Obtain time intensity curves (TICs) by importing the DCE-CT data into software that provides the ability to identify a region of interest (ROI) within the tumor volume. Then calculate the mean CT enhancement in the ROI as a function of time. In this experiment custom software was developed to identify a ROI and calculate the TIC.
15. Obtain quantitative estimates of perfusion and vascular permeability by fitting measured TICs using a two-compartment tracer kinetic model. Fitting can be performed using DCE-CT analysis software and use the apriori estimates of the plasma volume fraction and interstitial volume fractions as fixed parameters in the two-compartment tracer kinetic model. Use previously reported methods to obtain apriori estimates of the plasma and interstitial volume fractions[14].

4. Spatial Measurements of Tumor Interstitial Fluid Pressure

1. To measure IFP connect the 25 G spinal needle to the pressure transducer and to the IFP acquisition system through 50 cm of PE20 polyethylene tubing. Flush the entire system with a heparin sulfate/saline solution (1:10). Sterilize the needle with 70% isopropyl before use.
2. Turn on the acquisition system and launch the IFP acquisition software and load the settings files to calibrate the system to acquire IFP measurements in mmHg. Click the acquire button to continuously collect IFP data.
3. Perform IFP measurements between 48 and 72 hr post-injection of CT-liposomes (this corresponds to the approximate time of peak accumulation of the CT-liposomes in the tumor), using the methods described in 4.8. Attach the IFP needle to the CT-IFP robot.
4. Perform calibration scans to align the coordinate systems for the CT-IFP robot and the CT scanner. Add the fiducial marker attachment to the CT-IFP robot and perform a four volumetric CT scan with the fiducial marker in four different positions.
    1. Launch the CT-IFP robot controller software, initialize the robot, and move the robot to the three positions by entering the x,y,z targeting positions and clicking the 'go' button.
    2. Take a CT scan at the following x,y,z coordinates: (1) 0,0,0; (2) -10,0,0; (3) 0,7,0; and (4) 0,0,10. Select a 90 kV, 10 mA, 16 sec scan using the CT-scanner software and press 'Start' to initiate the scan. Reconstruct the scan as described in 3.10.

5. Launch the CT-IFP robot alignment software. Click the 'add' button loaded in the 'Registration Data' region and select the four reconstructed registration scans obtained in 4.3, then click 'open'.
    NOTE: The pixel location of the fiducial marker will automatically be entered into the software.
    1. Click the 'Calculate Transform' button and then click the 'Apply Transform' button. This generates alignment data that will be used to convert the CT-IFP robot coordinate system to the CT scanner coordinate system. After the calibration is complete, attach the animal platform to the CT-IFP robot.

6. Anesthetize each mouse using 2% isoflurane mixed with medical air or oxygen and confirm by pinching the toe and observing no reaction. Immobilize animal on the CT-IFP robot platform and position the mouse such that the tumor is accessible to the CT-IFP robot system. Immobilize the tumor using tape such that it does not move during IFP needle insertion.
7. Perform an anatomic micro-CT scan prior to inserting the IFP needle. Reconstruct the CT data using the steps described in 3.10.
8. Load the pre-needle insertion CT data into the CT-IFP robot alignment software. Adjust the window and level to visualize the tumor. Click on the rim of the tumor in any image, then click on a second rim location.
    NOTE: The software will calculate a series of positions along a linear line between the two positions. Note the x, y and z coordinates for a series of 5 to 8 evenly spaced positions from the list.
9. Prepare the IFP system by flushing the needle with heparin saline solution prior to insertion.
10. Enter the first pre-determined needle positions into the x,y,z, into the CT-IFP robot control software and press-move to 'go' button to move the robot to the desired position. Click the 'Insert Needle' button to insert the needle into the tissue.
    1. After inserting the needle ensure good fluid communication between the IFP needle and the tissue by pinching and releasing the PE20 tubing, noting that the IFP measurement increases and returns to pre-pinching value on the IFP acquisition software. Reject measurements that do not return to baseline.

11. Acquire an anatomic CT scan with the needle inserted, then click the 'Retract Needle' button on the CT-IFP robot control software to retract the needle from the tissue. Reject any IFP measurements where the IFP value does not return to the pre-needle insertion value after

withdrawal of the needle. This signifies the needle may have been clogged during the measurement. Repeat steps 4.8 to 4.10 for each needle position.

12. Determine the needle position within the tumor volume by calculating the x, y, and z positions of the needle port relative to the center of mass of the tumor volume as identified in the post-insertion volumetric CT scan of the needle.

13. Return animals to their cage after all measurements are complete. Do not leave animals unattended, and take care to observe them until consciousness has been regained and they are able to maintain sternal recumbency.
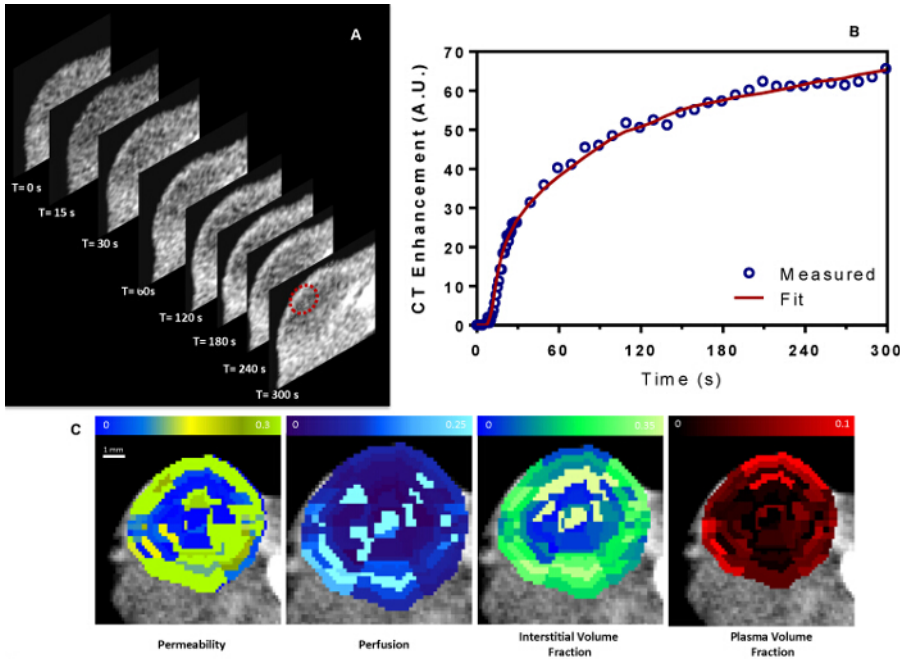
Representative Results

The aforementioned protocol should yield CT-liposomes with an encapsulated concentration of iohexol, mean liposome diameter, and zeta potential of 55 mg ml^{-1}, 91.8 ± 0.3 nm and -45.5 ± 2.5 mV, respectively. **Figure 1a** includes representative DCE-CT imaging results, yielding a time series of volumetric data that show the temporal changes in intra-tumoral accumulation of iohexol. Selecting a ROI within the tumor yields a TIC that can be quantified using tracer kinetic modeling methods to obtain estimates of perfusion, vascular permeability, plasma volume fraction, and interstitial volume fraction (**Figure 1b**). In this study, a two-compartment tracer kinetic model was used and fit to the measured TIC using a non-linear curve fitting routine implemented in Matlab[14]. Segmenting the tumor volume into multiple regions of interest of equal size allows for quantification of the spatial distribution of haemodynamic parameters within the tumor volume (**Figure 1c**). Segmentation can be performed either manually, which is time consuming and difficult, or automatically as performed here using an algorithm that divides the tumor in multiple equal sized ROIs using a spherical coordinate system. The DCE-CT methods provide quantitative estimates of the spatial distribution of perfusion, vascular permeability, plasma volume fraction, and interstitial volume fraction. These parameters were observed to be spatially heterogeneous with higher levels of perfusion, plasma and interstitial volume fractions along the periphery compared to the central tumor volume.
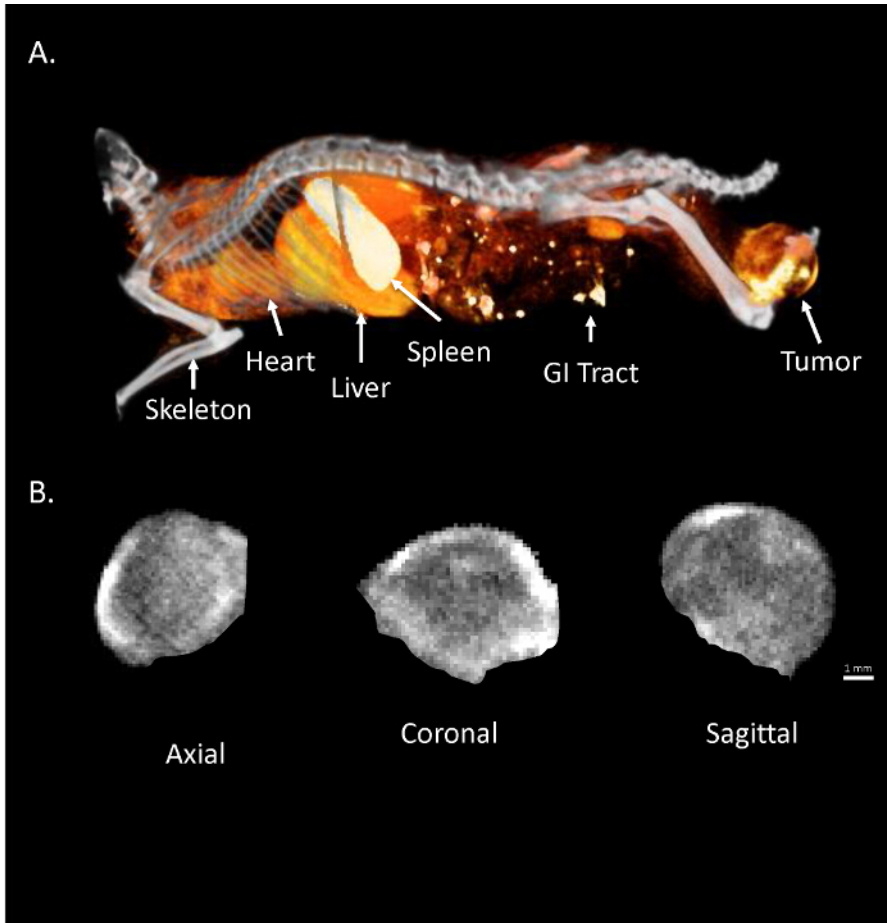
The volumetric CT imaging method reveals the biodistribution and intra-tumoral distribution of CT-liposomes. **Figure 2a** shows the biodistribution of CT-liposomes at 48 hr post-injection. The agent is still circulating in the vascular system, with substantial uptake observed in the spleen and liver. The intra-tumoral accumulation of CT-liposomes was observed to be heterogeneous, with predominantly peripheral accumulation compared to the center, as denoted by the bright regions within the tumor volume (**Figure 2b**).

Volumetric CT imaging can be used to track the location of IFP measurements made using the CT-IFP robot setup. **Figure 3a** shows the placement of the IFP needle within the tumor volume as imaged using high-resolution micro-CT. The needle can clearly be identified within the tumor volume allowing for spatial localization of the IFP measurements within the tumor volume (**Figure 3b**). It is possible to generate a spatial map of IFP throughout the tumor by performing multiple IFP measurements within the tumor volume. The spatial IFP can then be correlated with the corresponding measurements of tumor microcirculation and CT-liposome accumulation.

Volumetric CT imaging allows for a common frame of reference making it possible to co-localize measurements of haemodynamics, IFP, and CT-liposome accumulation. **Figure 4** gives an example of spatially co-localized measurements of CT-liposome accumulation, IFP, perfusion, vascular permeability, plasma volume fraction, and interstitial volume fraction. It was observed that perfusion and the plasma volume fraction was significantly correlated with the intra-tumoral accumulation of CT-liposomes in subcutaneous MDA-MB-231 tumors. Furthermore, the radial distribution of IFP correlated with haemodynamic measurements. These results suggest a complex spatio-temporal relationship exists between the tumor microcirculation, IFP and the intra-tumoral accumulation of liposomes[14].

Figure 1: DCE-CT Imaging of the Tumor Microcirculation. (a) A representative series of temporal CT images collected within the tumor volume, depicting the contrast agent kinetics as a function of time. The red contour represents a ROI where the time intensity curve (TIC) is measured. (**b**) The TIC is fit using a two-compartment tracer kinetic model to yield quantitative estimates of haemodynamic parameters within the ROI. (**c**) Representative spatial distribution of quantitative haemodynamic parameters in the tumor. Please click here to view a larger version of this figure.

Figure 2: Volumetric CT-Imaging of Liposome Accumulation. (**a**) A representative 3D volume-rendered image demonstrating the biodistribution of CT-liposomes. (**b**) Representative axial, coronal, and sagittal slices taken through the center of the tumor showing the intra-tumoral accumulation of CT-liposomes at 48 hr post-injection. Please click here to view a larger version of this figure.
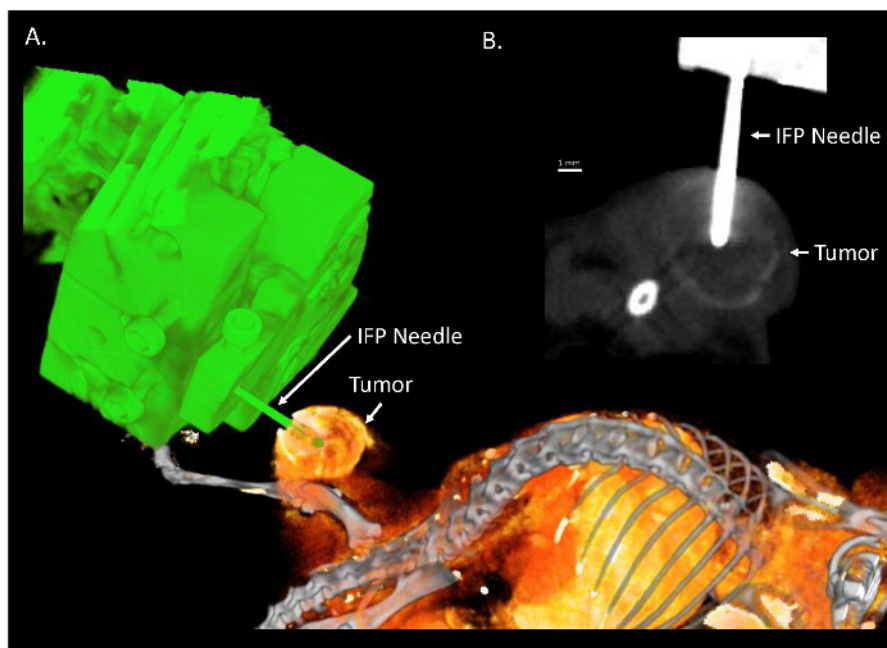
Figure 3: Image Guided IFP Measurements. (**a**) A representative 3D volume-rendered image of the CT-IFP robot system (green) post-needle insertion into a subcutaneous tumor at 48 hr post-injection of CT-liposomes (orange). (**b**) A representative CT image of the post-needle insertion. Please click here to view a larger version of this figure.
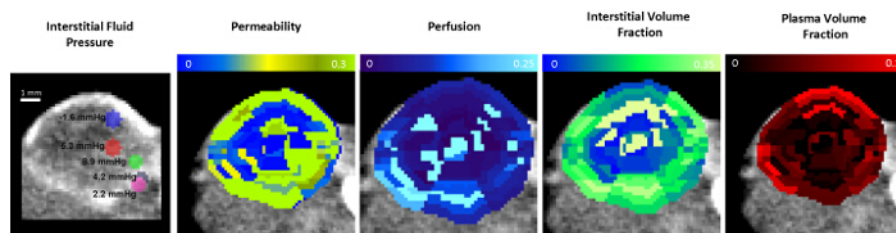
Figure 4: Co-localized Measurements of Tumor Microcirculation, IFP, and CT-liposome accumulation. Panel showing a representative spatial co-localization of CT-liposome accumulation taken 48 hr post-injection, IFP, perfusion, vascular permeability, plasma volume fraction and interstitial volume fraction. Re-print with permission from[14]. Please click here to view a larger version of this figure.

Discussion

The methods for image-based measurement presented herein enable determination of the spatial distribution of tumor microcirculation properties, IFP, and CT-liposome accumulation. Previous attempts to relate these properties have relied on performing bulk measurements across multiple tumor-bearing animals and therefore lack the sensitivity to elucidate mechanisms responsible for heterogeneity in intra-tumoral accumulation that has commonly been observed for nano-sized drug delivery systems[15]. DCE-CT provides a tool to measure the intra-tumoral variations in properties of the tumor microcirculation, volumetric CT provides an accurate depiction of CT-liposome deposition kinetics, and the CT-IFP robot system provides a tool to perform spatial mapping of IFP in the same animal. Furthermore, DCE-CT imaging is a clinically approved method for measuring tumor hemodynamics in the clinical setting, making the findings of this study potentially clinically translatable.

Given the complexity of the measurements, there are several critical factors to ensure the collection of robust data sets. DCE-CT based quantification of the tumor microcirculation is arguably the most difficult to ensure accurate estimates of tumor haemodynamics. It requires obtaining TICs with high signal to noise ratios (SNR) and employing a robust fitting algorithm to quantify the TICs[16,17]. Visual inspection of TICs can be used to remove low SNR data from the analysis. Furthermore, if care is not taken then the fitting of high SNR TICs may also lead to erroneous estimates of tumor perfusion, vascular permeability, plasma volume fraction, and interstitial volume fraction[16]. In order to maximize quantification accuracy a strategy was employed to obtain model independent estimates of the plasma and interstitial volume fractions, which are subsequently used as fixed parameters during the model fit of measured TICs. This method ensures robust estimates of tumor perfusion and vascular permeability are obtained[15].

Robust analysis of the intra-tumoral distribution of CT-liposomes requires performing volumetric CT imaging after sufficient accumulation of the agent. From previous studies, the peak tumor accumulation of CT-liposomes occurs between 48 to 72 hr in mouse xenografts[3,15]. Furthermore a linear relationship exists between CT-liposome concentration and contrast enhancement in CT imaging allowing for simple quantification of the variations in intra-tumoral accumulation of CT-liposomes[15].

Accurate measurements of IFP using the needle-based method require good fluid communication between the catheter and the tissue. Furthermore, it is important to only use tumors that have high central tumor IFP (>5 to 10 mmHg), otherwise there will be minimal spatial variations in IFP. Spatial measurements of IFP using the CT-IFP robot systemcan be challenging due to tissue motion caused by needle insertion. Imaging pre- and post-needle placement is crucial for accurately identifying the needle placement; however, it can be difficult to relate the position between subsequent needle placements due to tissue warping between measurements. It was found that randomly choosing needle positions results in significant tissue deformation during needle insertion. As a result, this method provided the least accurate spatial mapping of IFP. Conversely, performing measurements along a linear track across the tumor volume and inserting the needle tangential to the track can improve the spatial accuracy of IFP measurements. Inserting the needle tangential to the track minimizes the effects of tissue deformation along the measurement track direction.

This study demonstrated the ability to measure the spatial distribution of tumor microcirculation, IFP and CT-liposome accumulation in an individual tumor. After mastering these techniques, it is then possible to perform these measurements independently or together to characterize the tumor microenvironment and its effects on drug delivery. Using these methods in the MDA-MB-231 breast xenograft model revealed that perfusion and plasma volume fraction are strong mediators of the intra-tumoral distribution of liposomes[14]. There was not found to be a strong relationship between IFP and liposome distribution. However, IFP was strongly correlated to measurements of tumor perfusion, suggesting that IFP may play an indirect role in mediating liposome distribution through modulation of blood flow.

Disclosures

The authors have nothing to disclose

Acknowledgements

References

1. Seo, J. W., Zhang, H., Kukis, D. L., Meares, C. F., & Ferrara, K. W. A novel method to label preformed liposomes with 64Cu for positron emission tomography (PET) imaging. *Bioconjugate chemistry.* **19** (12), 2577-2584 (2008).
2. Huang, H., Dunne, M., Lo, J., Jaffray, D., & Allen, C. Comparison of Computed Tomography- and Optical Image-Based Assessment of Liposome Distribution. *Molecular Imaging.* **12** (3), 148-160 (2013).
3. Stapleton, S. *et al.* A mathematical model of the enhanced permeability and retention effect for liposome transport in solid tumors. *PloS one.* **8** (12), e81157 (2013).
4. Zheng, J. *et al.* A multimodal nano agent for image-guided cancer surgery. *Biomaterials.* **67** 160-168 (2015).
5. Zheng, J., Liu, J., Dunne, M., Jaffray, D. A., & Allen, C. In vivo performance of a liposomal vascular contrast agent for CT and MR-based image guidance applications. *Pharmaceutical research.* **24** (6), 1193-1201 (2007).
6. Harrington, K. J. *et al.* Effective targeting of solid tumors in patients with locally advanced cancers by radiolabeled pegylated liposomes. *Clinical Cancer Research.* **7** (2), 243-254 (2001).
7. Stapleton, S., Allen, C., Pintilie, M., & Jaffray, D. A. Tumor perfusion imaging predicts the intra-tumoral accumulation of liposomes. *J Control Release.* **172** (1), 351-357 (2013).
8. Lammers, T., Kiessling, F., Hennink, W. E., & Storm, G. Nanotheranostics and image-guided drug delivery: current concepts and future directions. *Mol. Pharm.* **7** 1899-1912 (2010).
9. Stapleton, S., & Milosevic, M. F. in *Cancer Targeted Drug Delivery.* 241-272 Springer, (2013).
10. Blanco, E., Shen, H., & Ferrari, M. Principles of nanoparticle design for overcoming biological barriers to drug delivery. *Nature biotechnology.* **33** (9), 941-951 (2015).
11. Heldin, C. H., Rubin, K., Pietras, K., & Ostman, A. High interstitial fluid pressure - an obstacle in cancer therapy. *Nat Rev Cancer.* **4** (10), 806-813 (2004).
12. Chauhan, V. P., Stylianopoulos, T., Boucher, Y., & Jain, R. K. Delivery of molecular and nanoscale medicine to tumors: transport barriers and strategies. *Annual review of chemical and biomolecular engineering.* **2** 281-298 (2011).
13. Bax, J. S. *et al.* 3D image-guided robotic needle positioning system for small animal interventions. *Medical physics.* **40** (1), 011909 (2013).
14. Stapleton, S., Milosevic, M., Tannock, I. F., Allen, C., & Jaffray, D. A. The intra-tumoral relationship between microcirculation, interstitial fluid pressure and liposome accumulation. *Journal of Controlled Release.* **211** 163-170 (2015).
15. Stapleton, S., Allen, C., Pintilie, M., & Jaffray, D. A. Tumor perfusion imaging predicts the intra-tumoral accumulation of liposomes. *J Control Release.* **172** (1), 351-357 (2013).
16. Brix, G., Zwick, S., Kiessling, F., & Griebel, J. Pharmacokinetic analysis of tissue microcirculation using nested models: multimodel inference and parameter identifiability. *Medical physics.* **36** (7), 2923-2933 (2009).
17. Brix, G., Griebel, J., Kiessling, F., & Wenz, F. Tracer kinetic modelling of tumour angiogenesis based on dynamic contrast-enhanced CT and MRI measurements. *European journal of nuclear medicine and molecular imaging.* **37** (1), 30-51 (2010).